Articles

Physical Society of Indonesia

Journal of the Physical Society of Indonesia **2(2)**, 134-144 (2026)

https://doi.org/10.35895/jpsi.2.2.134-144.2026

Carbonization of *Ageratum conyzoides* Leaves and Characterization for Supercapacitor Active Electrode Performance

Muhammad Ikram Handaru Putra, Bidayatul Armynah, Arifin Arifin, Dahlang Tahir*

Department of Physics, Faculty of Mathematics and Natural Sciences, Hasanuddin University, Makassar, 90245, Indonesia

(Received July 20, 2026; revised October 30, 2026; accepted October 31, 2026; published online November 01, 2026)

This study evaluated the viability of the invasive weed *Ageratum conyzoides* as a carbon precursor for supercapacitor electrodes. The research aimed to determine the optimal carbonization temperature for maximizing the specific capacitance. The biomass underwent chemical activation using 0.3 M KOH. Subsequently, the samples were carbonized in an N_2 atmosphere at varying temperatures (600, 700, and 800°C) and physically activated with CO_2 at 800°C. Structural and morphological characterizations using thermogravimetric analysis (TG-DTG), X-ray diffraction (XRD), Fourier transform infrared (FTIR) spectroscopy, and scanning electron microscopy (SEM) confirmed the successful decomposition of organic components into a highly porous amorphous carbon network. An increase in the carbonization temperature directly correlated with a reduction in material density, indicating enhanced pore formation. Electrochemical measurements via cyclic voltammetry in a 1 M H_2SO_4 electrolyte revealed that the electrode carbonized at 800°C delivered a maximum specific capacitance of 75.97 F/g, compared to 58.21 F/g and 40.09 F/g for the 600°C and 700°C variants, respectively. These findings established both the ecological and technical potential of converting an invasive weed into functional energy storage materials.

Keywords: *Ageratum conyzoides, activated carbon, supercapacitor, carbonization, cyclic voltammetry*

This is an open access article under the CC BY-NC license.
Copyright © 2026 by Author. Published by Physical Society of Indonesia

1. INTRODUCTION

The global energy transition from fossil fuels to renewable sources necessitates the development of highly reliable energy storage systems to mitigate the intermittent nature of solar and wind power (Feng & Lazkano, 2025; Gielen et al., 2019). Among various technologies, supercapacitors have emerged as highly promising candidates due to their superior power density, exceptional cycle life, and favorable safety characteristics compared to conventional batteries (Gopi & Ramesh, 2024; Taer et al., 2021). The electrochemical performance of supercapacitors relies heavily on their electrode materials. Biomass-derived activated carbon has gained significant attention as an electrode precursor due to its low production cost, renewability, and naturally advantageous hierarchical porous architecture (Shrestha, 2025; Zhang et al., 2022).

Despite the exploration of biomasses, Ageratum conyzoides (commonly known as bandotan) has received limited attention as a precursor for supercapacitor applications. *A. conyzoides* is an invasive weed distributed across tropical regions, causing agricultural losses and ecological disruptions (Batish et al., 2006; Kaur et al., 2012). Utilizing this invasive weed offers a circular economy approach by converting an ecological liability into a high-value technological asset. Previous studies on plants from the same Asteraceae family, such as sunflower and Parthenium hysterophorus, yielded activated carbons with specific capacitances up to 691 F/g (El-Hofy et al., 2025; Komal et al., 2023). However, the application of *A.conyzoides* for electrical double-layer capacitor (EDLC) electrodes has not been established in the studies reviewed.

To develop an optimal porous structure for ion accumulation, a combination of chemical and physical activation is essential. Potassium hydroxide (KOH) is widely recognized for its efficacy in

*Contact Author: dtahir@fmipa.unhas.ac.id

developing microporosity, whereas thermal carbonization in a nitrogen (N_2) atmosphere followed by physical activation using carbon dioxide (CO_2) maximizes overall pore development (Bejjanki et al., 2023; Jaliaz & Awitdrus, 2025). Therefore, this study investigated the carbonization of *A. conyzoides* leaves at varying temperatures (600°C, 700°C, and 800°C) to determine the optimal thermal condition. The structural transformations, pore development, and their direct impact on the electrochemical performance of the resulting electrodes were systematically evaluated.

2. METHOD

The fabrication of supercapacitor electrodes from *Ageratum conyzoides* (bandotan) leaves involved a systematic sequence of procedures: precursor preparation, chemical activation, pelletization, high-temperature carbonization, and physical activation. Following the material synthesis, the obtained carbon pellets were assembled into a symmetrical electrical double-layer capacitor (EDLC) cell to evaluate their electrochemical performance. The comprehensive experimental workflow for this research is systematically illustrated in Figure 1.

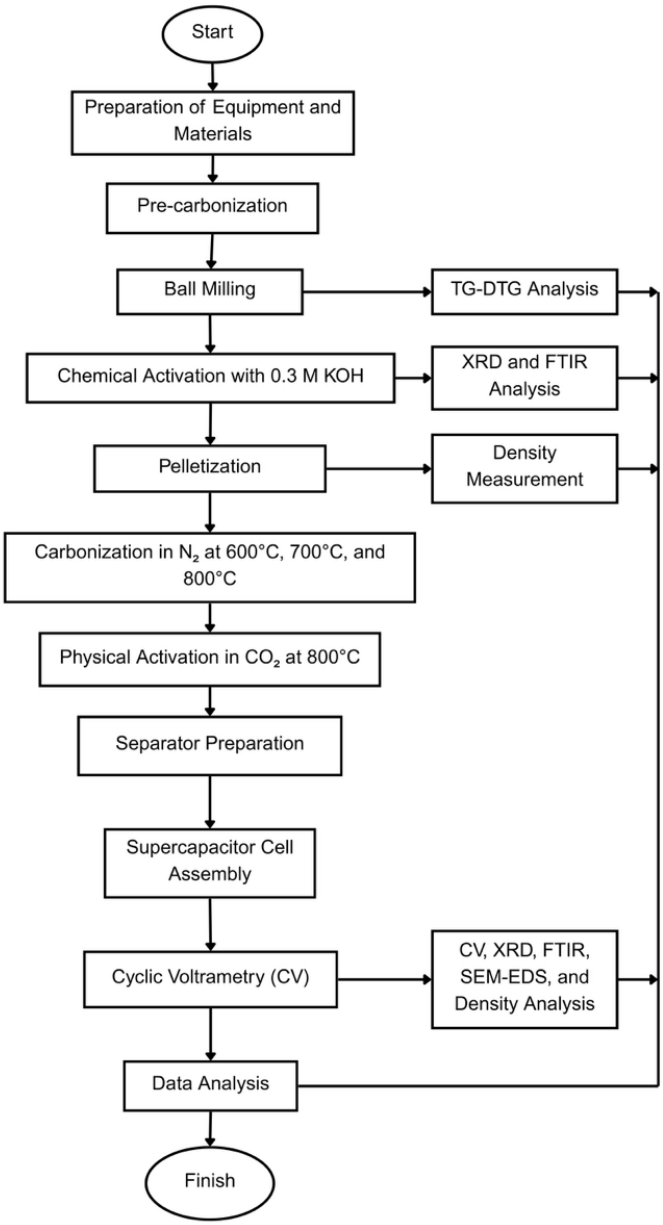


Figure 1. Flowchart of the experimental procedure for synthesizing *A. conyzoides* activated carbon.

2.1. Biomass Preparation and Pre-carbonization

The initial phase involved the collection of fresh *A. conyzoides* leaves, which were subsequently washed with distilled water to remove external impurities and dust. The cleaned leaves were dried naturally under direct sunlight for 2 to 3 days. A total of 400 g of the sun-dried leaves was divided into 10 equal batches (40 g per batch) and subjected to a pre-carbonization process. This process was carried out in an oven at 150°C for 1 hour to significantly reduce the moisture content and initiate the degradation of light volatile compounds. After cooling to room temperature, the pre-carbonized biomass was crushed using a mechanical blender and sifted through a 200-mesh sieve to obtain a uniform and fine precursor powder (Armynah et al., 2023; 2024; 2025; 2026).

2.2. Chemical Activation and Pelletization

Chemical activation was employed using potassium hydroxide (KOH) to facilitate the initial development of microporosity within the carbon matrix. The activating agent was prepared by dissolving 2.52 g of KOH in 150 mL of distilled water. This solution was heated to 80°C and continuously stirred using a magnetic stirrer at 400 rpm for 1 hour. Subsequently, 30 g of the sieved precursor powder was slowly added into the 0.3 M KOH solution. The mixture was homogenized using a magnetic stirrer at a higher speed of 800 rpm for 2 hours to ensure optimal chemical impregnation. The resulting slurry was then dried in an oven at 75–80°C for 8 hours, finely ground using a mortar, and re-sieved through a 200-mesh screen.

To fabricate the solid electrodes, 0.7 g of the chemically activated powder was transferred into a cylindrical mold and compressed using a hydraulic press under a pressure of 80.64 kPa for 5 minutes. The precise mass, thickness, and diameter of the resulting solid pellets were recorded using a digital balance and a digital caliper (Armynah et al., 2023; 2024; 2025; 2026).

2.3. Carbonization and Physical Activation

Carbonization was conducted to decompose the remaining organic frameworks, such as cellulose and lignin, into a stable carbon structure. The carbon pellets were placed in a high-temperature tube furnace and heated under a continuous nitrogen (N_2) gas flow. To investigate the effect of thermal treatment, the carbonization was performed at varying target temperatures of 600°C, 700°C, and 800°C for 1 hour.

Immediately following the carbonization phase at each respective temperature, the N_2 gas flow was terminated. The atmosphere was then substituted with carbon dioxide (CO_2) gas at a constant flow for physical activation at 800°C for 1 hour. This secondary activation aimed to expand the existing pores and increase the specific surface area of the electrodes. After the furnace naturally cooled to room temperature, the activated carbon pellets were mechanically polished using P1200-grit sandpaper to achieve uniform dimensions with a thickness of approximately 0.2 mm and a diameter of 8 mm (Armynah et al., 2023; 2024; 2025; 2026).

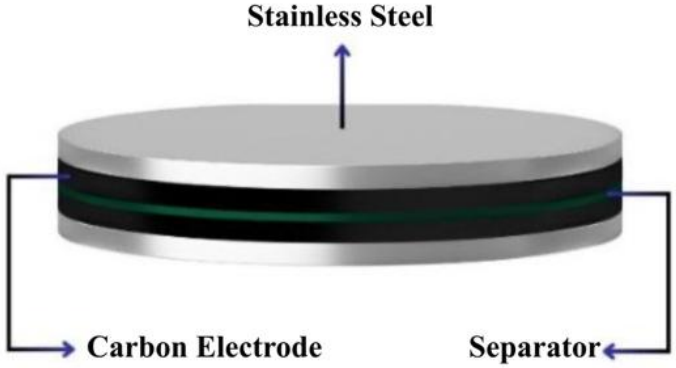


Figure 2. Schematic design of the assembled symmetrical supercapacitor cell.

2.4. Separator Preparation and Supercapacitor Cell Assembly

A natural and cost-effective separator was fabricated utilizing duck eggshell membranes. The eggshells were initially cleaned with distilled water, placed in a beaker, and immersed in distilled water

containing 10 to 15 drops of 1 M HCl solution. The mixture was stirred and left undisturbed for approximately 24 hours until the inner membranes naturally detached from the calcium carbonate shells. The extracted membranes were washed thoroughly with distilled water until a neutral pH was achieved, and subsequently cut to match the dimensions of the supercapacitor electrodes (Armynah et al., 2023; 2024; 2025; 2026).

Prior to cell assembly, the activated carbon electrodes were soaked in a 1 M H_2SO_4 aqueous electrolyte solution for 48 hours to guarantee deep ionic penetration into the porous carbon network. As illustrated in Figure 2, a symmetrical EDLC cell was constructed by sandwiching the eggshell membrane separator between two identical carbon electrodes. These components were tightly compressed between stainless steel current collectors, which were pre-shaped to match the electrode dimensions, and secured using paper clips to maintain excellent interfacial contact.

2.5. Material Characterization and Electrochemical Measurements

The thermal degradation profile of the raw *A. conyzoides* biomass was investigated using Thermogravimetry and Differential Thermogravimetry (TG-DTG) to determine the optimal pyrolysis temperature ranges. The electrode density (ρ)ρ before and after the carbonization process was calculated by dividing the measured mass (m) by the cylindrical volume (V) of the pellets. The structural transformation and phase purity were analyzed using X-ray diffraction (XRD). The evolution of surface functional groups was evaluated via Fourier transform infrared (FTIR) spectroscopy within the wavenumber range of 500–4000 cm^{-1}. Morphological observation and elemental composition mapping were performed using scanning electron microscopy coupled with Energy Dispersive X-ray Spectroscopy (SEM-EDS).

The electrochemical properties of the assembled supercapacitor cells were quantitatively evaluated using a cyclic voltammetry (CV) instrument (Physics CV UR Rad-Er 5841). The CV measurements were carried out in a two-electrode configuration using a 1 M H_2SO_4 electrolyte within a stable potential window of 0.1 to 1.0 V at a constant scan rate of 1 mV/s. The specific capacitance (C_{sp}) of the supercapacitor cells was calculated from the generated cyclic voltammograms using the following Equation (1) (Armynah et al., 2023; 2024; 2025; 2026):

$$C_{sp} = \frac{I_c - I_d}{s \times m} \quad (1)$$

where Csp represents the specific capacitance (F/g), Ic is the charge current (A), I_d is the discharge current (A), s denotes the applied scan rate (V/s), and m is the total mass of the two carbon electrodes (g).

3. RESULTS AND DISCUSSION

3.1 Thermal Degradation Behavior

As illustrated in Figure 3, the thermal degradation profile of the A. conyzoides precursor was evaluated using TG-DTG analysis to determine the precise temperature dynamics during the carbonization process. The thermogravimetric (TG) curve revealed a distinctive three-stage mass loss mechanism characteristic of lignocellulosic biomass. The initial stage exhibited a 10.27% mass reduction up to 116.4°C, corresponding to the thermal dehydration and evaporation of physically adsorbed surface water. The second stage demonstrated a 29.28% mass loss up to 283.3°C, which is primarily attributed to the preliminary decomposition of hemicellulose and the initiation of cellulose breakdown. The most substantial mass reduction of 56.63% occurred in the third stage up to 317.3°C, signifying the severe structural decomposition of the primary biomass constituents, including the remaining cellulose and lignin networks (Armynah et al., 2023; 2024; 2025; 2026).

The derivative thermogravimetric (DTG) curve further corroborated these findings by displaying a prominent maximum degradation peak at 312.2°C, reaching a degradation rate of 0.0954 mg/min. Thermal conversion of lignocellulosic biomass has also been discussed in the carbon-material literature (Bejjanki et al., 2023; Zhang et al., 2022). This sharp single peak indicates that the most

intensive thermal decomposition occurred at this specific temperature, which is consistent with substantial degradation of cellulose-rich biomass.

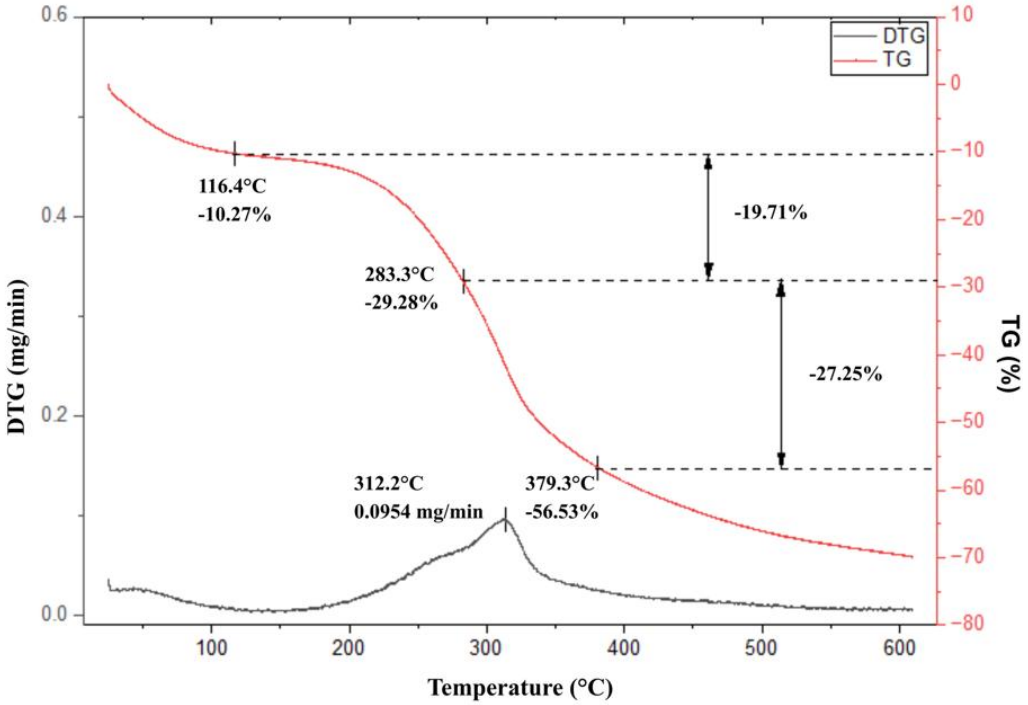


Figure 3. TG-DTG curves of the A. conyzoides precursor.

3.2 Physical Properties and Density Analysis

The density of a carbon electrode serves as a critical physical indicator of its internal porosity and potential charge storage capacity. A lower bulk density may indicate greater void volume, although surface area and pore-size distribution require independent measurements for electrolyte ion accumulation. To evaluate this, the physical dimensions (mass, thickness, and diameter) of the *A. conyzoides* pellets were systematically measured before and after the pyrolysis process at varying nitrogen temperatures (600, 700, and 800°C).

As summarized in Table 1, the uncarbonized solid precursor pellets exhibited relatively high initial densities of 0.90, 0.87, and 0.90 g/cm³ for the designated target temperatures of 600, 700, and 800°C, respectively. Following the thermal treatment, the pellets underwent significant dimensional and mass shrinkage due to the aggressive elimination of residual moisture and the volatilization of light organic compounds. Consequently, the final densities of the carbonized electrodes decreased substantially to 0.65, 0.61, and 0.55 g/cm³ for the samples treated at 600, 700, and 800°C, respectively.

Comparable biomass-derived supercapacitor electrodes have been investigated by Komal et al. (Komal et al., 2023) and Sahoo and Sahoo (Shrestha, 2025), although their processing conditions differ from those used here. This consistent density reduction trend is consistent with greater mass loss and potentially increased porosity at higher carbonization temperatures. The lowest density observed at the 800°C variant (0.55 g/cm³) suggests a more porous carbon structure, which requires direct porosity measurements to confirm, which theoretically aligns with superior electrochemical performance for supercapacitor applications (Armynah et al., 2023; 2024; 2025; 2026).

Table 1. Electrode densities before and after carbonization.

Carbonization Temperature (°C)	Density Before Pyrolysis (g/cm³)	Density After Pyrolysis (g/cm³)
600	0.90	0.65
700	0.87	0.61
800	0.90	0.55

3.3 Surface Chemical Properties (FTIR Analysis)

Fourier Transform Infrared (FTIR) spectroscopy was utilized in the wavenumber range of 500–4000 cm^{-1} to identify the evolution of surface functional groups before and after the carbonization process. The FTIR spectra presented in Figure 4 revealed a crucial chemical transformation from an aliphatic-rich biomass precursor into a conductive aromatic carbon network. Prior to pyrolysis, the precursor exhibited prominent aliphatic C–H stretching (2978.09 and 2873.94 cm^{-1}) and bending (1425.40 cm^{-1} vibrations. Following the thermal treatment, the intensity of these aliphatic peaks decreased significantly, indicating the massive degradation of volatile compounds and saturated hydrocarbons (Armynah et al., 2023; 2024; 2025; 2026).

Conversely, the carbonization process induced a substantial intensification of the conjugated C=C double bond peak at 1641.42 cm^{-1} (shifted from a weak peak at 1654.92 cm^{-1}). The emergence of this strong aromatic ring structure, resembling graphitic-like layers, is highly desirable for supercapacitor applications as it provides adequate pathways for electron delocalization, thereby potentially supporting electronic transport.

Furthermore, the partial carbonization strategically retained crucial oxygen functionalities, evidenced by the persistent broad O–H absorption band at 3412.08 cm^{-1}. This retained hydroxyl group may improve surface wettability (wettability) to the electrode surface, facilitating the penetration of the aqueous electrolyte into the carbon micropores. The retention of oxygen is also suggested by the peak splitting phenomenon in the C–O fingerprint region, where a single peak at 1076.28 cm^{-1} split into multiple sharp peaks (1246.02, 1153.43, 1097.50, and 1033.85 cm^{-1}) due to the selective decomposition of cellulose and lignin. The coexistence of these multi-oxygen groups (C–O and O–H) not only broadens ion accessibility but also may contribute to surface redox reactions at the electrode-electrolyte interface, generating a pseudocapacitance effect that may influence the overall specific capacitance (Armynah et al., 2023; 2024; 2025; 2026).

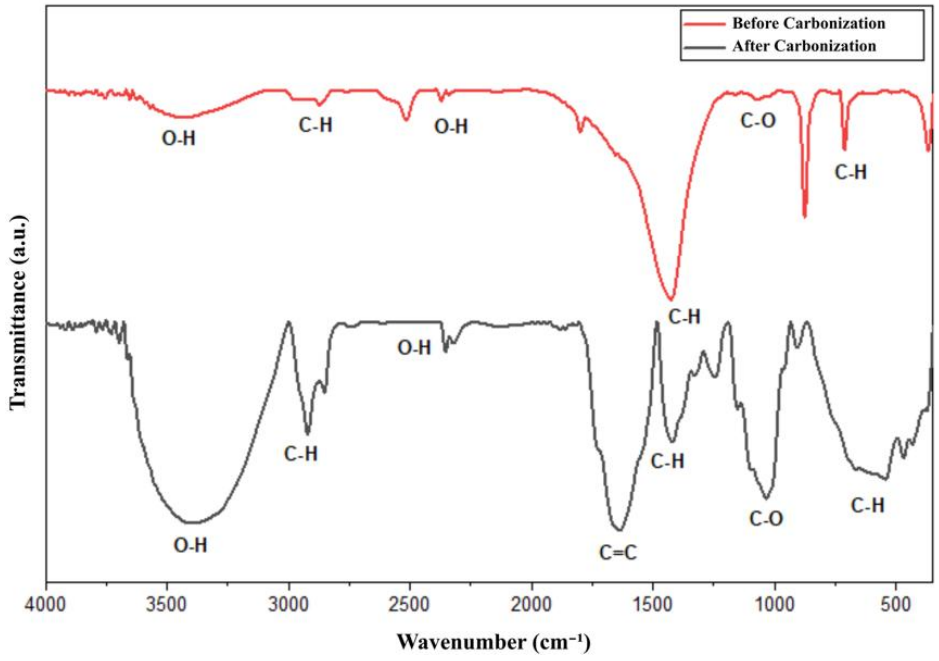


Figure 4. FTIR spectra of A. conyzoides before and after carbonization.

3.4 Structural and Phase Analysis (XRD)

X-ray Diffraction (XRD) analysis was performed to monitor the crystallographic transformations of the *A. conyzoides* biomass induced by the thermal and chemical treatments. As depicted in the diffractogram in Figure 5, two sharp, high-intensity crystalline peaks were observed at $2\theta \approx 44°$ and 64°, which require phase identification before assignment to specific inorganic minerals.

Upon undergoing pyrolysis in an N_2 atmosphere and KOH activation, these initial crystalline peaks completely degraded. The post-pyrolysis diffractogram displayed significantly broadened peaks

with low intensity, consistent with the formation of predominantly disordered carbon with a low degree of graphitization. In the context of energy storage, this predominantly amorphous nature is highly advantageous. The disordered structure represents looser interlayer spacing between the carbon sheets, which intrinsically promotes the development of high porosity and low density. This abundant void volume serves as active sites that facilitate rapid electrolyte ion penetration and mobility, thereby potentially supporting charge accumulation via the EDLC mechanism (Armynah et al., 2023; 2024; 2025; 2026).

Additionally, minor sharp peaks, labeled as residual phases, were detected in the activated sample. These features may originate from oxidized natural minerals or trapped potassium compounds from the KOH activator. The presence of these alkali metal compounds during the high-temperature treatment could contribute, as they act as internal etching agents that continuously disrupt the carbon framework to generate a rich microporous network on the electrode surface (Armynah et al., 2023; 2024; 2025; 2026).

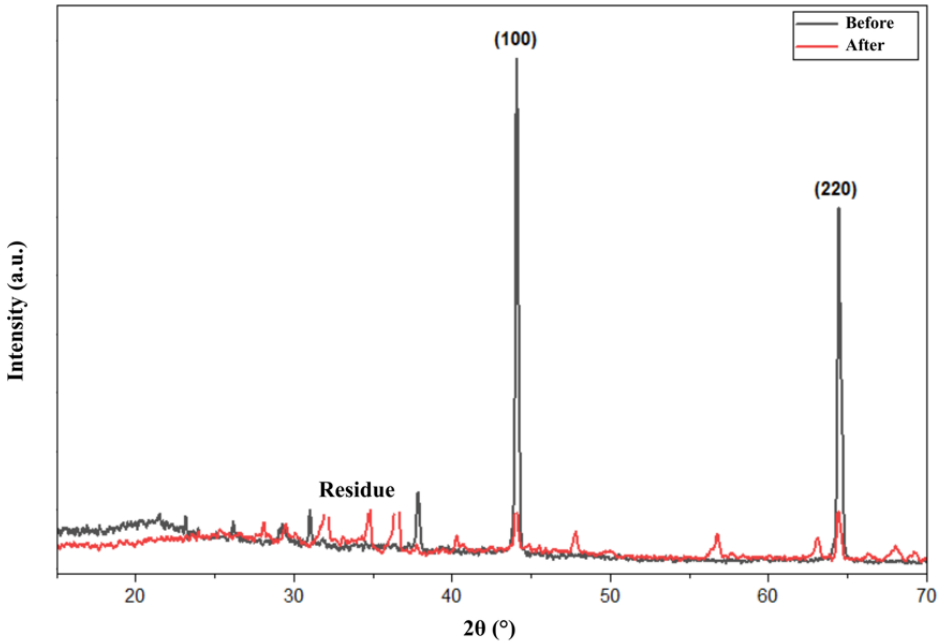


Figure 5. XRD patterns of the precursor and synthesized activated carbon.

3.5 Morphological and Elemental Composition (SEM-EDS)

Scanning Electron Microscopy (SEM) was utilized to visually evaluate the surface topography and surface morphology of the activated carbon electrodes. The SEM micrographs shown in Figure 6, obtained at magnifications of 10,000× and 40,000×, revealed a non-homogeneous, highly irregular porous architecture. The prominent cavities observed on the surface indicate that the applied pyrolysis process may have removed the internal organic compounds of the biomass, leaving behind a structurally expanded carbon matrix.

Image-based surface measurements indicated pore-like features (diameter $\geq 0.05\ \mu$m), with pore sizes ranging from 0.21 to 0.41 μm at 10,000× magnification and more defined pores of 0.07 to 0.18 μ m at 40,000× magnification. These surface features may be relevant for energy storage applications, as they act as primary reservoirs that minimize ion diffusion resistance and maximize the interfacial contact area between the solid electrode and the liquid electrolyte (Armynah et al., 2023; 2024; 2025; 2026).

Energy Dispersive X-ray Spectroscopy (EDS) was concurrently performed to quantify the elemental composition of the sample. As depicted in Figure 7 and Table 2, the EDS spectrum indicated that carbon (C) was the most dominant element, accounting for 52.07 wt% (74.45 at%), which substantiates the successful conversion of the biomass precursor into a solid carbon framework. Notably, Potassium (K) was detected at a significant concentration of 11.63 wt%. This residual potassium

originated from the KOH activating agent and is consistent with the use of KOH in activation in the chemical etching process that generated the observed porosity. Furthermore, the detection of Oxygen (O) at 4.69 wt% is consistent with the FTIR interpretation regarding the presence of hydrophilic surface functional groups (C–O and O–H). Trace amounts of other elements (Mg, Si, Al, Cl, Fe, Ca) were also identified, which are attributed to the inherent natural minerals present in the *A. conyzoides* weed (Armynah et al., 2023; 2024; 2025; 2026).

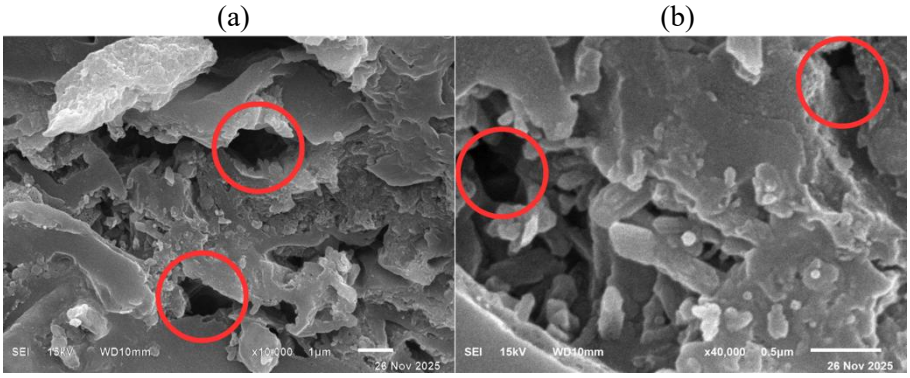


Figure 6. SEM micrographs of A. conyzoides-derived activated carbon at (a) 10,000× and (b) 40,000×.

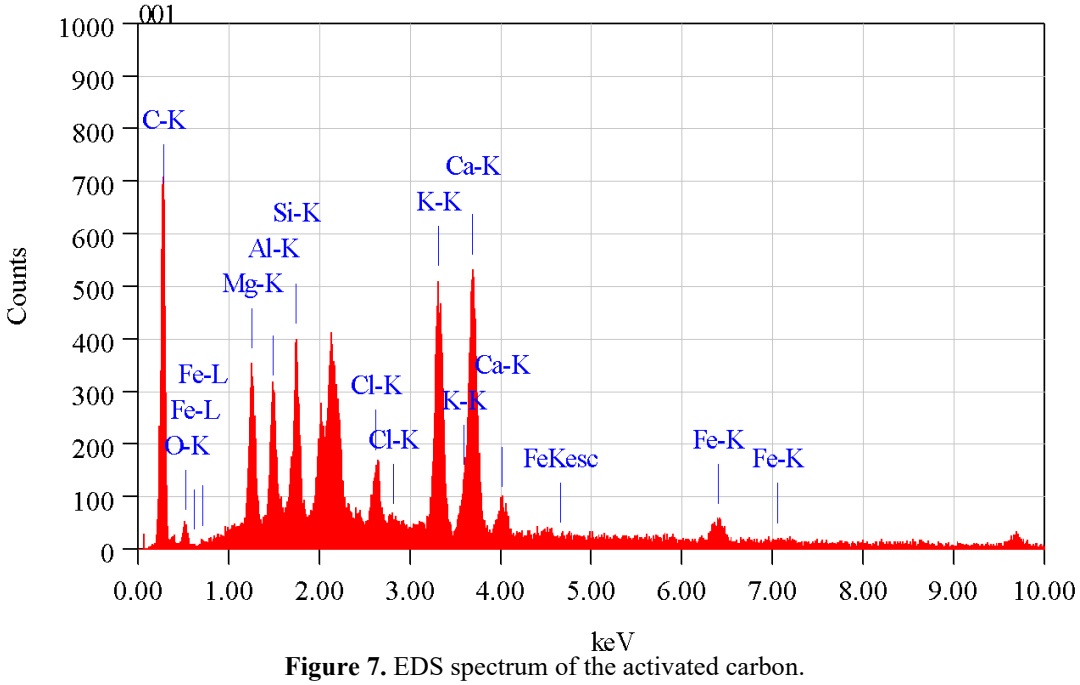


Figure 7. EDS spectrum of the activated carbon.

Table 2. EDS elemental composition of A. conyzoides-derived activated carbon.

Element	Weight Percentage (wt%)	Atomic Percentage (at%)
Carbon (C)	52.07	74.45
Oxygen (O)	4.69	5.03
Magnesium (Mg)	3.52	2.49
Aluminum (Al)	2.92	1.86
Silicon (Si)	3.76	2.30
Chlorine (Cl)	2.20	1.07
Potassium (K)	11.63	5.11
Calcium (Ca)	14.87	6.37
Iron (Fe)	4.34	1.32

3.6 Electrochemical Performance (Cyclic Voltammetry)

The fundamental charge storage capability of the assembled supercapacitor cells was evaluated using cyclic voltammetry (CV) at a constant scan rate of 1 mV/s. Figure 8 illustrates the CV voltammograms of the electrodes carbonized at 600, 700, and 800 °C. All curves exhibited a quasi-rectangular and highly symmetrical shape lacking prominent redox peaks. This profile is consistent with predominantly electric double-layer charge storage; the CV data alone do not establish the absence of faradaic contributions (Armynah et al., 2023; 2024; 2025; 2026).

The integrated area under the CV curve directly correlates to the total charge stored by the electrode. The specific capacitance (C_{sp}) values calculated from the cyclic voltammograms are systematically presented in Table 3.

Table 3. Specific capacitance at different carbonization temperatures.

Carbonization Temperature (°C)	Total Mass (g)	Specific Capacitance (F/g)
600	0.054	58.21
700	0.051	40.09
800	0.038	75.97

Related studies of biomass-derived electrodes report that activation and precursor chemistry can affect electrochemical performance (Armynah et al., 2024; 2025; Taer et al., 2021). The electrochemical evaluation revealed that the carbonization temperature affected the final capacitance. The electrode pyrolyzed at 800 °C exhibited the widest enclosed CV area and delivered a maximum specific capacitance of 75.97 F/g. This superior performance is consistent with the previous density analysis, where the 800°C variant possessed the lowest density, and although the pore structure was not quantified. The enhanced porosity effectively accommodated a larger volume of H_2SO_4 electrolyte ions, thereby maximizing the total charge storage capacity of the *A. conyzoides* derived.

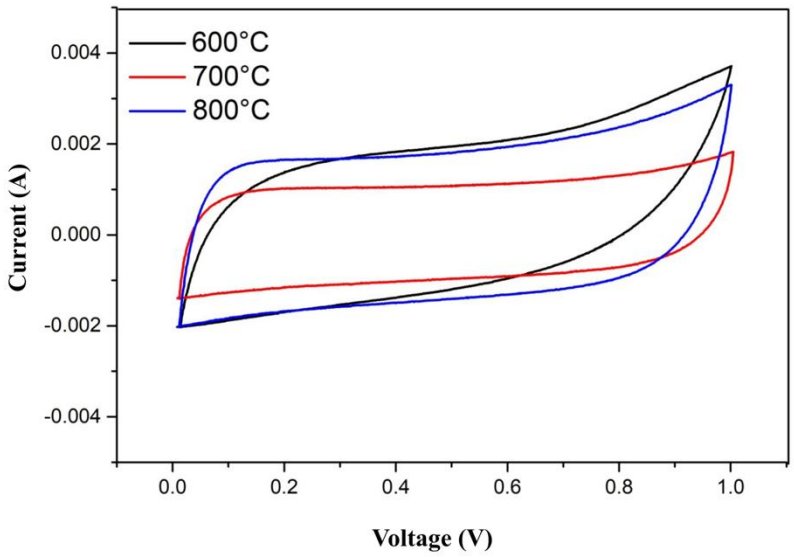


Figure 8. Cyclic voltammograms of supercapacitor cells prepared at different carbonization temperatures (1 mV/s).

4. CONCLUSION

This study successfully demonstrated the viability of utilizing the invasive weed *Ageratum conyzoides* as a sustainable and low-cost carbon precursor for supercapacitor electrodes. Through chemical activation with 0.3 M KOH and high-temperature carbonization in a nitrogen atmosphere, the

biomass was effectively transformed into a predominantly disordered carbon structure with visible surface pores. Structural and morphological characterizations (FTIR, XRD, and SEM-EDS) indicated decomposition of organic components, the formation of a stable aromatic structure, and the development of a heterogeneous macroporous surface enriched with oxygen functional groups and residual potassium.

The electrochemical evaluation showed an association between the carbonization temperature, material density, and charge storage capacity. The electrode pyrolyzed at 800 °C exhibited the lowest measured bulk density, specifically the lowest density and the highest observed specific capacitance of 75.97 F/g in a 1 M H_2SO_4 electrolyte. These findings suggest that *A. conyzoides* holds significant potential as a renewable and functional energy storage material, simultaneously offering a technological approach to mitigating an ecological liability. Future research should focus on optimizing the activation parameters and utilizing advanced characterizations, such as the Brunauer-Emmett-Teller (BET) and Galvanostatic Charge-Discharge (GCD) methods, to further comprehensively enhance and evaluate the supercapacitor's performance.

ACKNOWLEDGMENTS

The authors acknowledge the Department of Physics, Faculty of Mathematics and Natural Sciences, Hasanuddin University, and the Materials Physics Laboratory, Universitas Riau, for providing laboratory facilities, instrumentation, and technical support for this research.

AUTHOR CONTRIBUTIONS

Conceptualization, B.A. and M.I.H.P.; methodology, M.I.H.P.; software, D.T.; validation, D.T. and M.I.H.P.; formal analysis, B.A.; investigation, M.I.H.P.; resources, M.I.H.P.; data curation, M.I.H.P.; writing—original draft preparation, M.I.H.P.; writing—review and editing, visualization, A.A.; supervision, B.A. All authors must review and approve their contributions before publication.

FUNDING

This research received no external funding.

DATA AVAILABILITY STATEMENT

The data supporting the findings of this study are available from the corresponding author upon reasonable request.

CONFLICTS OF INTEREST

The authors declare no conflicts of interest.

ARTIFICIAL INTELLIGENCE (AI) USAGE DECLARATION

AI-assisted tools were used for language editing and editorial proofreading. The authors remain responsible for the accuracy, originality, and integrity of the manuscript.

REFERENCES

Armynah, B., Erwinda, E., Agustino, A., Taer, E., Mahmud, S., & Tahir, D. (2023). Biowaste-derived oxygen-self-doped three-dimensional interconnected porous carbon for electrochemical supercapacitor applications. Energy Sources, Part A: Recovery, Utilization, and Environmental Effects, 45(2), 6331–6342. https://doi.org/10.1080/15567036.2023.2215198

Armynah, B., Nairanti, D., Agustino, A., Taer, E., & Tahir, D. (2024). Discarded Persea americana leaf-derived natural O, Mg, and Ca self-doped activated carbon and its applications as electrode materials for high-

performance symmetric supercapacitors. Diamond and Related Materials, 143, 110879. https://doi.org/10.1016/j.diamond.2024.110879

Armynah, B., Sari, S. I., Agustino, A., Taer, E., & Tahir, D. (2025). Tetra-heteroatom natural-doped activated carbon derived from cocoa leaf waste for advanced symmetric supercapacitors. Journal of Power Sources, 642, 236947. https://doi.org/10.1016/j.jpowsour.2025.236947

Armynah, B., Ayad Muayyad, A. M., Agustino, A., Taer, E., Apriwandi, A., Ismardi, A., Fathona, I. W., Rosi, M., Haryanti, N. H., Suryajaya, S., Isnasyauqiah, I., Usman, I., Julnaidi, J., Taslim, R., & Tahir, D. (2026). Heteroatom self-doped activated carbon from Moringa seed shells via KOH/CO_2 double activation for high-performance supercapacitors. Advanced Powder Technology, 37(11), 105427. https://doi.org/10.1016/j.apt.2026.105427

Batish, D. R., Singh, H. P., Kohli, R. K., & Kaur, S. (2006). Ageratum conyzoides: A noxious weed. In Invasive Plants: Ecological Threats and Management Options. Wiley-VCH.

Bejjanki, D., Banothu, P., Kumar, V. B., & Kumar, P. S. (2023). Biomass-derived N-doped activated carbon from Eucalyptus leaves as an efficient supercapacitor electrode material. C, 9(1), 24. https://doi.org/10.3390/c9010024

El-Hofy, M. S., Ebrahim, S., Ali, A. E., Elasala, G. S., & Sakr, A.-H. (2025). Supercapacitor electrode fabricated by activated carbon obtained from peels of sunflower seeds (Helianthus annuus L.). Chemistry Research Journal, 10(2), 35–46.

Feng, S., & Lazkano, I. (2025). Energy storage and clean energy transitions. Energy Policy, 198, 114447. https://doi.org/10.1016/j.enpol.2024.114447

Gielen, D., Boshell, F., Saygin, D., Bazilian, M. D., Wagner, N., & Gorini, R. (2019). The role of renewable energy in the global energy transformation. Energy Strategy Reviews, 24, 38–50. https://doi.org/10.1016/j.esr.2019.01.006

Gopi, C. V. V. M., & Ramesh, R. (2024). Review of battery-supercapacitor hybrid energy storage systems for electric vehicles. Results in Engineering, 24, 103598. https://doi.org/10.1016/j.rineng.2024.103598

Jaliaz, A., & Awitdrus, A. (2025). Making supercapacitor carbon electrodes from lemongrass leaf biomass with variations in physical activation temperature. Komunikasi Fisika Indonesia, 22(1), 49–52. https://doi.org/10.31258/jkfi.22.1.49-52

Kaur, S., Batish, D. R., Kohli, R. K., & Singh, H. P. (2012). Ageratum conyzoides: An alien invasive weed in India. In J. R. Bhatt, J. S. Singh, S. P. Singh, R. S. Tripathi, & R. K. Kohli (Eds.), Invasive alien plants: An ecological appraisal for the Indian subcontinent (pp. 57–76). CABI.

Komal, Kumar, A., Kumar, Y., & Shukla, V. K. (2023). Parthenium hysterophorus derived activated carbon for EDLC device application. Journal of Materials Science: Materials in Electronics, 34(28), 1880. https://doi.org/10.1007/s10854-023-11309-6

Shrestha, D. (2025). High-performance supercapacitor electrodes from optimized single-step carbonized Michelia champaca biomass. Journal of Environmental & Earth Sciences, 7(6), 1–22. https://doi.org/10.30564/jees.v7i6.8444

Taer, E., Apriwandi, A., Andani, D. R., & Taslim, R. (2021). Solid coin-like design activated carbon nanospheres derived from shallot peel precursor for boosting supercapacitor performance. Journal of Materials Research and Technology, 15, 1732–1741. https://doi.org/10.1016/j.jmrt.2021.09.025

Zhang, W., Qiu, X., Wang, C., Zhong, L., Fu, F., Zhu, J., Zhang, Z., Qin, Y., Yang, D., & Xu, C. C. (2022). Lignin derived carbon materials: Current status and future trends. Carbon Research, 1(1), 14. https://doi.org/10.1007/s44246-022-00009-1